2012 IEEE International Conference on Systems, Man, and Cybernetics
October 14-17, 2012, COEX, Seoul, Korea

A Robust On-line Learning Algorithm for Type-2 Fuzzy Neural Networks and its Experimental Evaluation on an Autonomous Tractor

Erdal Kayacan, Erkan Kayacan, Herman Ramon and Wouter Saeys
Division of Mechatronics, Biostatistics and Sensors (MeBioS),
Department of Biosystems (BIOSYST), KU Leuven
Kasteelpark Arenberg 30, B-3001, Heverlee (Leuven), Belgium
E-mail: {erdal.kayacan, erkan.kayacan, herman.ramon, wouter.saeys}@biw.kuleuven.be

***Abstract*—Production machines, especially in agriculture, with higher efficiencies will be very important in the future because of the limited agricultural areas in the world and the high energy and labor costs. In order to increase the capacity of agricultural machinery, one can think to further increase the size of the machines. However, the limits in this direction will soon be reached as there is a maximum size to still allow road transport. On the other hand, energy costs are constantly increasing, such that the energy use should be minimized. A better option would be to use advanced learning algorithms, which can learn the system dynamics online, for the control of the production machines in order to increase their effectiveness. In this study, a Takagi-Sugeno-Kang type-2 fuzzy neural network with a sliding mode control theory-based learning algorithm is proposed for the control of the yaw dynamics of an autonomous tractor which includes various uncertainties, disturbances and nonlinearities, especially coming from the hydraulic sub systems. Experimental results show the efficacy and the efficiency of the proposed learning algorithm.**

***Index Terms*—Sliding mode control, type-2 fuzzy logic systems, type-2 fuzzy neural networks, autonomous tractor**

I. Introduction

Since autonomous agricultural production machines have complex structures and vaguely known dynamics, it is generally a challenging task to control them using conventional controllers, *e.g.* PID controllers. The use of conventional controllers for the control of agricultural production machines has three basic disadvantages:

1) Well tuning of the controller coefficients is a difficult task: Since an accurate mathematical model of an autonomous production machine is difficult to obtain, the usage of analytical methods to calculate the controller coefficients is almost impossible. Trial-and-error method is usually preferred in real-time applications.
2) Adaptability is a must: Even if it is assumed that the correct controller coefficients are found, uncertainties and time varying parameters coming from the biological variability and changing environmental conditions make the control performance worse, because conventional controllers cannot adapt themselves to changing conditions.
3) Subsystems are in interaction with each other: Production machines usually consist of many subsystems which are always in interaction with each other. In the case of using independent conventional controllers for each subsystem, well tuning of the controller coefficients is a challenging task because the output of one controller always affects controllers of the other subsystems.

The drawbacks of conventional control algorithms mentioned above, which result in suboptimal efficiency of the controlled autonomous production machines, can be solved by the introduction of learning behavior in machine controllers. In other words, the control parameters should be consequently adapted in accordance with the changing conditions. In this study, a Takagi-Sugeno-Kang (TSK) type-2 fuzzy neural network (T2FNN) with a sliding mode control (SMC) theory-based learning algorithm is proposed for the control of the yaw dynamics of an autonomous tractor which includes various uncertainties, disturbances and nonlinearities.

Type-2 fuzzy logic systems (T2FLSs) were introduced by Zadeh in 1975 and improved by Mendel and Karnik in [1], [2]. T2FLSs have been suggested to be a more promising method than their type-1 counterparts for handling uncertainties such as noisy data and changing environments [3], [4]. In [5] and [6], the effects of the measurement noise in type-1 and type-2 fuzzy logic controllers and identifiers have been simulated to perform a comparative analysis. In [7], it is concluded that the use of T2FLSs in real world applications which exhibit measurement noise and modeling uncertainties can be a better option than type-1 FLSs (T1FLSs). In [8], interval T2FLSs are presented for the problem of short term load forecasting, and it is shown that interval T2FLSs outperform the traditional T1FLSs in terms of generalization power and forecasting error. In [9], an interval type-2 TSK fuzzy logic controller for modular and reconfigurable robots is proposed. Real-time applications show that the developed controller can outperform some well-known linear and nonlinear controllers for different configurations.

Whereas the secondary membership functions can take values in the interval of [0,1] in generalized T2FLSs, they are uniform functions that only take on values of 1 in interval T2FLSs. Since the general T2FLSs are computationally very demanding (this is because the type-reduction is computationally expensive), the use of interval T2FLSs is more commonly seen in literature, due to the fact that the computations are more easily manageable. In an interval TSK T2FLS, there exists a design parameter that weights the sharing of lower and upper firing levels of each fired rule. That parameter can be tuned during the design of the TSK system. While [10] uses the least mean square method for finding the correct value of that parameter, an SMC theory-based learning algorithm is proposed for tuning that parameter in [11]. This paper presents the real time evaluation of the algorithm proposed in [11].

The main body of the paper contains five sections: In section II, the mathematical model of the tractor yaw dynamics is given. In Section III, the proposed sliding mode feedback-error-learning approach is presented, and the parameter update rules for T2FNNs are proposed for the triangular membership functions case. In Section IV, the real-time results are given. Finally, in Section V, conclusions are presented.

II. The Mathematical Model of The Yaw Dynamics of The Tractor

The velocities and the sideslip angles at the rigid body and the wheels of the tractor are presented in Fig. 1(a). Similarly, the forces at different locations of the tractor are shown in Fig. 1(b).

The lateral dynamics of the tractor can be written as follows [12]:

$$m(\dot{v}_c + u_c\gamma) = F_{t,f}\sin\delta + F_{l,f}\cos\delta + F_{l,r} \tag{1}$$

where m, v_c, u_c, γ, $F_{t,f}$, $F_{l,f}$, $F_{l,r}$ and δ represent the mass of the tractor, the lateral velocity of the center of gravity (CG), the longitudinal velocity of the CG, the yaw rate, the traction and lateral forces on the front wheel, the lateral force on the rear wheel, the steering angle of the front wheel, respectively.

The yaw dynamics of the tractor are written as follows:

$$I_z\dot{\gamma} \quad = \quad l_f(F_{t,f}\sin\delta + F_{l,f}\cos\delta) - l_r F_{l,r} \tag{2}$$

where l_f, l_r and I_z respectively represent the distance between the front axle and the center of gravity of the tractor, the distance between the rear axle and the center of gravity of the tractor, and the moment of inertia of the tractor.

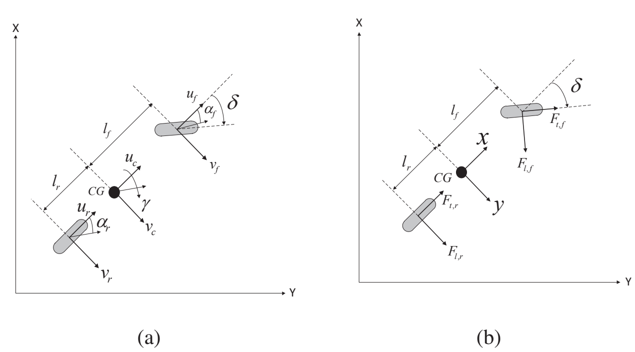

Fig. 1: Dynamic bicycle model for a tractor: (a) velocities and slip angles (b) forces at different locations of the system

The tire side slip angles must be calculated in order to determine the forces caused by the slip. It is assumed that the steering angle of the front wheel is small, and this allows to make the following approximations: $\sin\delta \approx \delta$ and $\cos\delta \approx 1$. The side slip angles of the front (α_f) and the rear tires (α_r) are written as follows:

$$\alpha_f = \frac{v_c + l_f\gamma}{u_c} - \delta \;\text{ and }\; \alpha_r = \frac{v_c - l_r\gamma}{u_c} \tag{3}$$

To determine the lateral force on the tire, there are many different approaches in literature. In this study, the lateral tire forces are calculated using a linear model which assumes these to be proportional to the slip angles in [13], [14]

$$F_{l,i} = -C_{\alpha,i}\alpha_i \qquad i = \{f, r\} \tag{4}$$

where $C_{\alpha,i}$, $i = \{f, r\}$, represents the cornering stiffness of the tires of the tractor. The tire cornering stiffness parameters are the averaged slopes of the lateral force characteristics in this method.

The equations of yaw motion of the autonomous tractor are written in state space form by combining (1), (2), (3) and (4) as follows:

$$\begin{bmatrix} \dot{v}_c \\ \dot{\gamma} \end{bmatrix} = \begin{bmatrix} A_{11} & A_{12} \\ A_{21} & A_{22} \end{bmatrix} \begin{bmatrix} v_c \\ \gamma \end{bmatrix} + \begin{bmatrix} B_1 \\ B_2 \end{bmatrix} u \tag{5}$$

where

$$\begin{aligned} A_{11} &= -\frac{C_{\alpha,f} + C_{\alpha,r}}{mu_c}, \\ A_{12} &= \frac{-l_f C_{\alpha,f} + l_r C_{\alpha,r}}{mu_c} - u_c, \\ A_{21} &= \frac{-l_f C_{\alpha,f} + l_r C_{\alpha,r}}{I_z u_c}, \\ A_{22} &= -\frac{l_f^2 C_{\alpha,f} + l_r^2 C_{\alpha,r}}{I_z u_c}, \\ B_1 &= \frac{C_{\alpha,f}}{m} \;,\; B_2 = \frac{l_f C_{\alpha,f}}{I_z} \\ u &= \delta(t) \end{aligned} \tag{6}$$

III. The Adaptive Fuzzy Neuro Control Approach

A. The control scheme

The proposed control scheme in this study is schematically illustrated in Fig. 2. This method was originally proposed in [15] for robot control in which a neural network works in parallel with a PD controller. The arrow in Fig. 2 indicates that the output of the PD controller is used to tune the parameters of the T2FNN.

The PD controller acts as an ordinary feedback controller to ensure the stability of the system and as an inverse reference model of the response of the system under control. The PD control law is described as follows:

$$\tau_c = k_P e + k_D \dot{e} \tag{7}$$

where $e = \gamma_{ref} - \gamma$ is the feedback error, γ_{ref} is the target value, k_P and k_D are the controller gains.

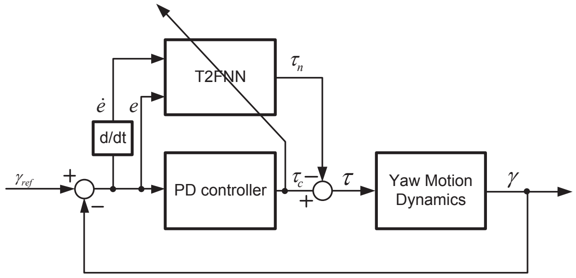

Fig. 2: Block diagram of the proposed adaptive fuzzy neuro scheme

B. Type-2 fuzzy neural network with triangular membership functions

The mathematical expression for the triangular membership function is expressed as:

$$\mu(x) = \begin{cases} 1 - \left|\frac{x-c}{d}\right| & |x-c| < d \\ 0 & otherwise \end{cases} \tag{8}$$

where c and d are the *center* and the *width* of the membership function, x is the input vector. In Figs. 3(a) and 3(b), triangular type-2 fuzzy membership functions with uncertain width and uncertain center are shown. In this study, a triangular type-2 fuzzy membership function with uncertain width and fixed center (Figs. 3(a)) is considered.

Each membership function in the antecedent part is represented by an *upper* and a *lower* membership function. They are denoted as $\overline{\mu}(x)$ and $\underline{\mu}(x)$. The strength of the rule R_{ij} is obtained as a T-norm of the membership functions in the premise part (by using a multiplication operator):

$$\underline{W_{ij}} = \underline{\mu}_{1i}(x_1)\underline{\mu}_{2j}(x_2) \tag{9}$$

$$\overline{W_{ij}} = \overline{\mu}_{1i}(x_1)\overline{\mu}_{2j}(x_2) \tag{10}$$

The triangular membership functions $\underline{\mu_{1i}(x_1)}$, $\overline{\mu_{1i}(x_1)}$, $\underline{\mu_{2j}(x_2)}$, and $\overline{\mu_{2j}(x_2)}$ of the inputs x_1 and x_2 in the above expression can be shown as follows:

$$\underline{\mu_{1i}(x_1)} = \begin{cases} 1 - \left|\frac{x_1 - \underline{c_{1i}}}{\underline{d_{1i}}}\right| & \left|x_1 - \underline{c_{1i}}\right| < \underline{d_{1i}} \\ 0 & otherwise \end{cases} \tag{11}$$

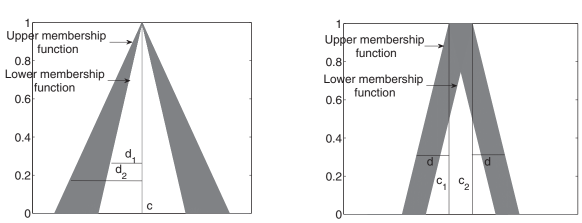

(a) (b)

Fig. 3: Type-2 fuzzy set with uncertain width (a) and uncertain center (b)

$$\overline{\mu_{1i}(x_1)} = \begin{cases} 1 - \left|\frac{x_1 - \overline{c_{1i}}}{d_{1i}}\right| & |x_1 - \overline{c_{1i}}| < \overline{d_{1i}} \\ 0 & otherwise \end{cases} \tag{12}$$

$$\underline{\mu_{2j}(x_2)} = \begin{cases} 1 - \left|\frac{x_2 - \underline{c_{2j}}}{\underline{d_{2j}}}\right| & \left|x_2 - \underline{c_{2j}}\right| < \underline{d_{2j}} \\ 0 & otherwise \end{cases} \tag{13}$$

$$\overline{\mu_{2j}(x_2)} = \begin{cases} 1 - \left|\frac{x_2 - \overline{c_{2j}}}{d_{2j}}\right| & \left|x_2 - \overline{c_{2j}}\right| < \overline{d_{2j}} \\ 0 & otherwise \end{cases} \tag{14}$$

C. Interval type-2 A2-CO Takagi-Sugeno-Kang (TSK) model

The interval TSK T2FLS considered in this paper uses type-2 triangular membership functions in the premise part and crisp numbers in the consequent part. This structure is called A2-C0 fuzzy system [16], and it is shown in Fig. 4. The fuzzy *if-then* rule R_{ij} of a $zero^{th}$-order type-2 TSK model with two input variables where the consequent part is a crisp number can be defined as follows:

$$R_{ij}: \text{ If } x_1 \text{ is } \tilde{A}_{1i} \text{ and } x_2 \text{ is } \tilde{A}_{2j}, \text{ then } f_{ij} = d_{ij} \tag{15}$$

The followings are the operations in each layer in Fig. 4: *Layer 1:* The input signals feed the system. *Layer 2:* For each input signal entering the system, the membership degrees $\underline{\mu}$ and $\overline{\mu}$ are determined. *Layer 3:* This layer calculates the firing strengths of the rules which are realized using the *prod* t-norm operator using (9) and (10). *Layer 4:* This layer determines the outputs of the linear functions f_{ij} $(i = 1,\dots,I$ and $j = 1,\dots,J)$, in the consequent parts for the two inputs case.

$$f_{ij} = d_{ij} \tag{16}$$

Layer 5: This layer computes the product of the membership degrees $\underline{W_{ij}}$ and $\overline{W_{ij}}$ and linear functions f_{ij}. *Layer 6:* This layer includes two summation blocks. One of these blocks computes the sum of the output signals from layer 5 (the numerator part of (17)) and the other block computes the sum of the output signal of layer 3 (the denominator part of (17)). *Layer 7:* This layer calculates the output of the network using (18).

$$\tau_n = \int_{W_{11}\varepsilon[\underline{W}_{11},\overline{W}_{11}]} \cdots \int_{W_{IJ}\varepsilon[\underline{W}_{IJ},\overline{W}_{IJ}]} 1 \Big/ \frac{\sum_{i=1}^{I}\sum_{j=1}^{J} W_{ij}(x) f_{ij}}{\sum_{i=1}^{I}\sum_{j=1}^{J} W_{ij}(x)} \tag{17}$$

where f_{ij} is given by the *if-then* rule. The inference engine used in this paper replaces the type-reduction which is given as:

$$\tau_n = \frac{q\sum_{i=1}^{I}\sum_{j=1}^{J}\underline{W}_{ij}f_{ij}}{\sum_{i=1}^{I}\sum_{j=1}^{J}\underline{W}_{ij}} + \frac{(1-q)\sum_{i=1}^{I}\sum_{j=1}^{J}\overline{W}_{ij}f_{ij}}{\sum_{i=1}^{I}\sum_{j=1}^{J}\overline{W}_{ij}} \tag{18}$$

The design parameter, q, weights the sharing of lower and upper firing levels of each fired rule [16]. $\overline{W}_{ij}$ and $\underline{W}_{ij}$are determined using (9) and (10), and f_{ij} is determined using (16).

After the normalization of (18), the output signal of the T2FNN will acquire the following form:

$$\tau_n = q\sum_{i=1}^{I}\sum_{j=1}^{J} f_{ij}\underline{\widetilde{W_{ij}}} + (1-q)\sum_{i=1}^{I}\sum_{j=1}^{J} f_{ij}\overline{\widetilde{W_{ij}}} \tag{19}$$

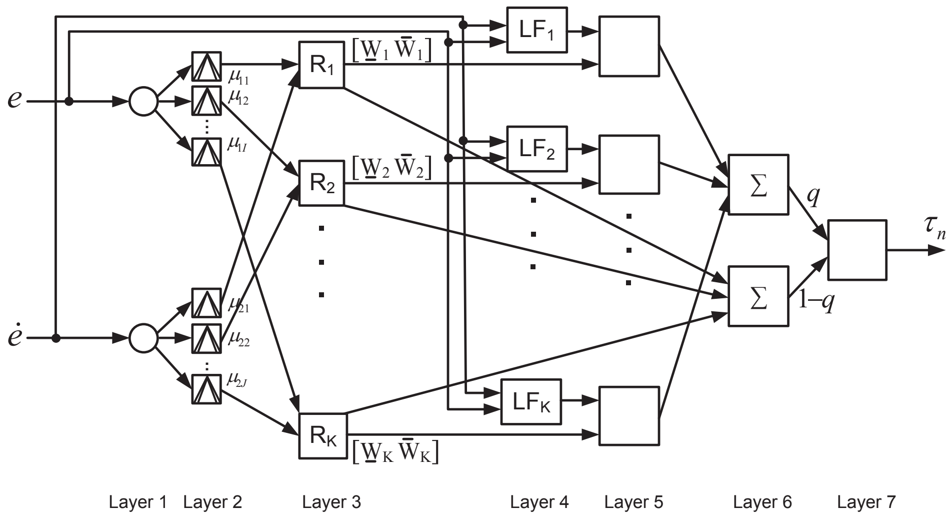

Fig. 4: Structure of T2FNN for two inputs

where $\widetilde{\underline{W_{ij}}}$ and $\widetilde{\overline{W_{ij}}}$ are the normalized values of the lower and the upper output signals of the neuron ij from the second hidden layer of the network:

$$\widetilde{\underline{W_{ij}}} = \frac{\underline{W_{ij}}}{\sum_{i=1}^{I}\sum_{j=1}^{J}\underline{W_{ij}}} \text{ and } \widetilde{\overline{W_{ij}}} = \frac{\overline{W_{ij}}}{\sum_{i=1}^{I}\sum_{j=1}^{J}\overline{W_{ij}}}$$

The following vectors have been specified:

$\underline{\widetilde{W}}(t) = \left[\widetilde{\underline{W_{11}}}(t)\ \widetilde{\underline{W_{12}}}(t) \ldots \widetilde{\underline{W_{21}}}(t)\ \ldots \widetilde{\underline{W_{ij}}}(t)\ \ldots \widetilde{\underline{W_{IJ}}}(t)\right]^T$

$\overline{\widetilde{W}}(t) = \left[\widetilde{\overline{W_{11}}}(t)\ \widetilde{\overline{W_{12}}}(t) \ldots \widetilde{\overline{W_{21}}}(t)\ \ldots \widetilde{\overline{W_{ij}}}(t)\ \ldots \widetilde{\overline{W_{IJ}}}(t)\right]^T$

$F = [f_{11}\ f_{12} \ldots f_{21} \ldots f_{ij} \ldots f_{IJ}]$

The following assumptions have been used in this investigation:

Both the input signals $x_1(t)$ and $x_2(t)$, and their time derivatives can be considered bounded:

$$|x_1(t)| \leq \widetilde{B}_x, \quad |x_2(t)| \leq \widetilde{B}_x \qquad \forall t \tag{20}$$

$$|\dot{x}_1(t)| \leq \widetilde{B}_{\dot{x}}, \quad |\dot{x}_2(t)| \leq \widetilde{B}_{\dot{x}} \qquad \forall t \tag{21}$$

where $\widetilde{B}_x$ and $\widetilde{B}_{\dot{x}}$ are assumed to be some known positive constants.

It is obvious that $0 < \widetilde{\underline{W_{ij}}} \leq 1$ and $0 < \widetilde{\overline{W_{ij}}} \leq 1$. In addition, it can be easily seen that $\sum_{i=1}^{I}\sum_{j=1}^{J}\widetilde{\underline{W_{ij}}} = \sum_{i=1}^{I}\sum_{j=1}^{J}\widetilde{\overline{W_{ij}}} = 1$. It is also considered that, τ and $\dot{\tau}$ will be bounded signals too, *i.e.*:

$$|\tau(t)| < B_\tau, \quad |\dot{\tau}(t)| < B_{\dot{\tau}} \quad \forall t \tag{22}$$

where B_τ and $B_{\dot{\tau}}$ are some known positive constants.

D. The sliding mode learning algorithm

Using the principles of SMC theory [17] the zero value of the learning error coordinate $\tau_c(t)$ can be defined as a time-varying sliding surface, *i.e.*:

$$S_c(\tau_n, \tau) = \tau_c(t) = \tau_n(t) + \tau(t) = 0 \tag{23}$$

which is the condition that the T2FNN is trained to become a nonlinear regulator to obtain the desired response during the tracking-error convergence movement by compensation for the nonlinearity of the controlled plant.

The sliding surface for the nonlinear system under control $S_p(e, \dot{e})$ is defined as:

$$S_p(e, \dot{e}) = \dot{e} + \chi e \tag{24}$$

with χ a positive constant determining the slope of the sliding surface.

Definition: A sliding motion will appear on the sliding manifold $S_c(\tau_n, \tau) = \tau_c(t) = 0$ after a time t_h, if the condition $S_c(t)\dot{S}_c(t) = \tau_c(t)\,\dot{\tau}_c(t) < 0$ is satisfied for all t in some non-trivial semi-open subinterval of time of the form $[t, t_h) \subset (0, t_h)$.

It is desired to devise a dynamical feedback adaptation mechanism, or online learning algorithm for the T2FNN parameters such that the sliding mode condition of the above definition is enforced.

E. The parameter update rules for T2FNN

The parameter update rules for a T2FNN which has two inputs are given in the following theorem.

Theorem 1: If the adaptation laws for the parameters of the considered T2FNN are chosen as:

$$\dot{\underline{c_{1i}}} = \begin{cases} \dot{\underline{c_{1i}}} = \dot{x}_1 & \left|x_1 - \underline{c_{1i}}\right| < \underline{d_{1i}} \\ 0 & otherwise \end{cases} \tag{25}$$

$$\overline{\dot{c}_{1i}} = \begin{cases} \overline{\dot{c}_{1i}} = \dot{x}_1 & |x_1 - \overline{c_{1i}}| < \overline{d_{1i}} \\ 0 & otherwise \end{cases} \tag{26}$$

$$\underline{\dot{c}_{2j}} = \begin{cases} \underline{\dot{c}_{2j}} = \dot{x}_2 & \left|x_2 - \underline{c_{2j}}\right| < \underline{d_{2j}} \\ 0 & otherwise \end{cases} \tag{27}$$

$$\overline{\dot{c}_{2j}} = \begin{cases} \overline{\dot{c}_{2j}} = \dot{x}_2 & \left|x_2 - \overline{c_{2j}}\right| < \overline{d_{2j}} \\ 0 & otherwise \end{cases} \tag{28}$$

$$\underline{\dot{d}_{1i}} = \underline{\mu_{1i}} \frac{-\alpha \underline{d_{1i}}^2}{x_1 - \underline{c_{1i}}} sgn(\tau_c) sgn\left(\frac{x_1 - \underline{c_{1i}}}{\underline{d_{1i}}}\right) \tag{29}$$

$$\overline{\dot{d}_{1i}} = \overline{\mu_{1i}} \frac{-\alpha \overline{d_{1i}}^2}{x_1 - \overline{c_{1i}}} sgn(\tau_c) sgn\left(\frac{x_1 - \overline{c_{1i}}}{\overline{d_{1i}}}\right) \tag{30}$$

$$\underline{\dot{d}_{2j}} = \underline{\mu_{2j}} \frac{-\alpha \underline{d_{2j}}^2}{x_2 - \underline{c_{2j}}} sgn(\tau_c) sgn\left(\frac{x_2 - \underline{c_{2j}}}{\underline{d_{2j}}}\right) \tag{31}$$

$$\overline{\dot{d}_{2j}} = \overline{\mu_{2j}} \frac{-\alpha \overline{d_{2j}}^2}{x_2 - \overline{c_{2j}}} sgn(\tau_c) sgn\left(\frac{x_2 - \overline{c_{2j}}}{\overline{d_{2j}}}\right) \tag{32}$$

$$\dot{f}_{ij} = -\frac{(q\underline{\widetilde{W}_{ij}} + (1-q)\overline{\widetilde{W}_{ij}})}{(q\underline{\widetilde{W}} + (1-q)\overline{\widetilde{W}})^T (q\underline{\widetilde{W}} + (1-q)\overline{\widetilde{W}})} \alpha sgn(\tau_c) \tag{33}$$

$$\dot{q} = -\frac{1}{F(\underline{\widetilde{W}} - \overline{\widetilde{W}})^T} \alpha sgn(\tau_c) \tag{34}$$

where α is a sufficiently large positive design constant satisfying the inequality:

$$\alpha > B_{\dot{\tau}} \tag{35}$$

then, given an arbitrary initial condition $\tau_c(0)$, the learning error $\tau_c(t)$ will converge firmly to zero during a finite time t_h.

Proof: The reader is referred to [11].

The relation between the sliding line S_p and the zero adaptive learning error level S_c is determined by the following equation:

$$S_c = \tau_c = k_D \dot{e} + k_P e = k_D \left(\dot{e} + \frac{k_p}{k_D} e\right) = k_D S_p \tag{36}$$

The tracking performance of the feedback control system can be analyzed by introducing the following Lyapunov function candidate:

$$V_p = \frac{1}{2} S_p^2 \tag{37}$$

Theorem 2: If the adaptation strategy for the adjustable parameters of the T2FNN is chosen as in (25)-(33), then the negative definiteness of the time derivative of the Lyapunov function in (37) is ensured.

Proof: The reader is referred to [11].

Remark: The obtained result means that, assuming the SMC task is achievable, using τ_c as a learning error for the T2FNN together with the adaptation laws (25)-(33) enforces the desired reaching mode followed by a sliding regime for the system under control.

IV. Experimental Results

A New Holland TZ25D tractor is equipped with necessary sensors and actuators as an experimental set-up (Fig. 5). The existing power steering unit has been replaced by an electro-hydraulic valve. The voltage and the rate of the steering angle are the input and the output for the adapted steering system. The valve characteristics are highly nonlinear and include a saturation as well as a dead-band region. The reference signal for the yaw rate is selected as a serial combination of a square, triangular and a sinusoidal wave along two periods for each.

The sampling time of the real-time set up is set to 50ms. The number of membership functions for the input 1 and input 2 is chosen as $I = J = 3$ for all simulations. The coefficients of the PD controller for the yaw motion dynamics have been tuned by trial-and-error, resulting in $k_p = 3$ and $k_d = 0.01$. The learning rate for the T2FNN is also tuned by using trial-and-error method which is equal to $\alpha = 2\text{x}10^{-3}$.

Fig. 5: Experimental set up

As can be seen from Fig. 6(a), when the PD controllers act alone, the control performance of yaw dynamics is not reasonable in which the PD controller gives a steady state error for the three different reference signals: square, triangular ana sinusoidal ones. The fine tuning of such controllers in real life is challenging, because in addition to the interactions of the subsystems, there exist unmodeled dynamics and uncertainties in real world applications. Figure 6(b) shows the case of the PD controller working in parallel with a T2FNN in which the control performance of the yaw dynamics is improved. These results indicate that the T2FNN is able to learn the system dynamics after a while, and it can improve the overall performance of the system without the need of fine tuning the conventional controller. Fig. 6(b) also shows that T2FNN gives slightly better performance when compared to T1FNN regarding the steady state error of the system.

Figure 7(a) shows the control signals coming from both the conventional PD controller and the T2FNN. As can be seen from Fig. 7(a), after a short time, the T2FNN is able to take over the control, thus becoming the leading controller. Figure 7(b) represents the online tuning of the parameter q in (18) which weights the sharing of lower and upper firing levels of each fired rule. Instead of using a constant value for the parameter q, this parameter has been tuned using an SMC theory-based learning algorithm, as explained in Section III E.

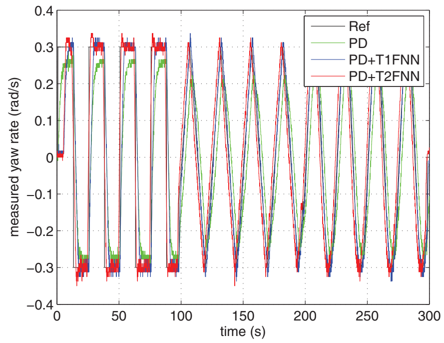

(a)

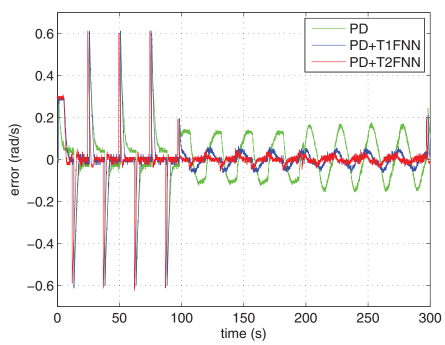

(b)

Fig. 6: The response of the yaw dynamics to different reference signals (a) and the corresponding tracking error (b)

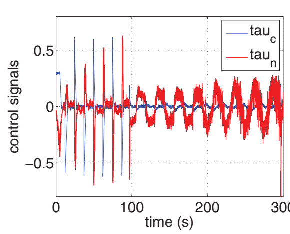

(a)

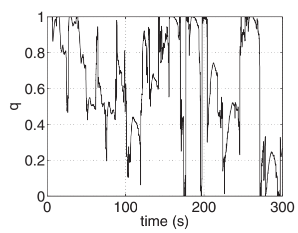

(b)

Fig. 7: Illustration of the input signals provided by the PD and T2FNN controllers (a) and the evolution of the tuning parameter q (b) over time for the reference signals presented in Fig. 6(a)

V. Conclusion

In an interval TSK T2FLS, there exists a design parameter that balances the sharing of lower and upper firing levels of each fired rule. That parameter can be tuned during the design of the TSK system. The novelty of this paper is that an SMC theory-based learning algorithm is proposed for tuning that parameter, which has been evaluated in real-time for control of the yaw dynamics of an autonomous tractor. The real-time results show that when the T2FNN is used in parallel with a conventional PD controller, the overall system learns the system dynamics to perform better performance in terms of a smaller settling time and zero steady state error. In addition to its well-known robustness property, another prominent feature is the computational simplicity of the proposed approach.

Acknowledgment

This work has been carried out within the framework of the LeCoPro project (grant nr. 80032) of the Institute for the Promotion of Innovation through Science and Technology in Flanders (IWT-Vlaanderen). Wouter Saeys is funded as a Postdoctoral Fellow of the Research Foundation - Flanders (FWO). We would like to thank Mr. Soner Akpinar for his technical support for the preparation of the experimental set up.

References

[1] N. N. Karnik, J. M. Mendel, and Q. Liang, "Type-2 fuzzy logic systems," *IEEE Trans. Fuzzy Syst.*, vol. 7, pp. 643–658, 1999.

[2] J. M. Mendel, R. John, and F. Liu, "Interval type-2 fuzzy logic systems made simple," *IEEE Trans. Fuzzy Syst.*, vol. 14, pp. 808–821, 2006.

[3] C.-F. Juang and C.-H. Hsu, "Reinforcement interval type-2 fuzzy controller design by online rule generation and q-value-aided ant colony optimization," *Systems, Man, and Cybernetics, Part B: Cybernetics, IEEE Transactions on*, vol. 39, no. 6, pp. 1528 –1542, dec. 2009.

[4] ——, "Reinforcement ant optimized fuzzy controller for mobile-robot wall-following control," *Industrial Electronics, IEEE Transactions on*, vol. 56, no. 10, pp. 3931 –3940, oct. 2009.

[5] R. Sepulveda, P. Melin, A. Rodriguez, A. Mancilla, and O. Montiel, "Analyzing the effects of the footprint of uncertainty in type-2 fuzzy logic controllers," *Engineering Letters*, vol. 13, pp. 138–147, 2006.

[6] M. A. Khanesar, M. Teshnehlab, E. Kayacan, and O. Kaynak, "A novel type-2 fuzzy membership function: Application to the prediction of noisy data," in *Computational intelligence for measurement system and applications*, sep. 2010, pp. 128 –133.

[7] M. Biglarbegian, W. Melek, and J. Mendel, "Design of novel interval type-2 fuzzy controllers for modular and reconfigurable robots: Theory and experiments," *Industrial Electronics, IEEE Transactions on*, vol. 58, no. 4, pp. 1371 –1384, april 2011.

[8] A. Khosravi, S. Nahavandi, D. Creighton, and D. Srinivasan, "Interval type-2 fuzzy logic systems for load forecasting: A comparative study," *Power Systems, IEEE Transactions on*, vol. PP, no. 99, p. 1, 2012.

[9] M. Biglarbegian, W. Melek, and J. Mendel, "Design of novel interval type-2 fuzzy controllers for modular and reconfigurable robots: Theory and experiments," *Industrial Electronics, IEEE Transactions on*, vol. 58, no. 4, pp. 1371 –1384, april 2011.

[10] T. Chen and Y.-C. Lin, "A fuzzy back-propagation-network ensemble with example classification for lot output time prediction in a wafer fab," *Applied Soft Computing*, vol. 2, pp. 658–666, 2009.

[11] E. Kayacan, W. Saeys, E. Kayacan, H. Ramon, and O. Kaynak, "Intelligent control of a tractor-implement system using type-2 fuzzy neural networks," in *IEEE WCCI 2012 - the 2012 IEEE World Congress on Computational Intelligence*, Brisbane, Australia, 10-15 June, 2012, pp. 171–178.

[12] M. Karkee and B. L. Steward, "Study of the open and closed loop characteristics of a tractor and a single axle towed implement system," *Journal of Terramechanics*, vol. 47, no. 6, pp. 379 – 393, 2010.

[13] D. Piyabongkarn, R. Rajamani, J. A. Grogg, and J. Y. Lew, "Development and experimental evaluation of a slip angle estimator for vehicle stability control," *IEEE Transactions on Control Systems Technologhy*, vol. 17, no. 1, pp. 78 – 88, 2009.

[14] C. Geng, L. Mostefai, M. Dena, and Y. Hori, "Direct yaw-moment control of an in-wheel-motored electric vehicle based on body slip angle fuzzy observer," *IEEE Transactions on Industrial Electronics*, vol. 56, no. 5, pp. 1411 – 1419, 2009.

[15] M. Kawato, Y. Uno, M. Isobe, and R. Suzuki, "Hierarchical neural network model for voluntary movement with application to robotics," *Control Systems Magazine, IEEE*, vol. 8, no. 2, pp. 8 –15, apr 1988.

[16] M. B. Begian, W. W. Melek, and J. M. Mendel, "Parametric design of stable type-2 TSK fuzzy systems," in *Proceedings of the North American Fuzzy Information Processing Systems*, 2008, pp. 1–6.

[17] V. I. Utkin, *Sliding Modes in Control Optimization*. Springer-Verlag, 1992.